Collisions of Slow Polyatomic Ions with Surfaces: Dissociation and Chemical Reactions of $C_2H_2^{+\bullet}$, $C_2H_3^+$, $C_2H_4^{+\bullet}$, $C_2H_5^+$, and Their Deuterated Variants $C_2D_2^{+\bullet}$ and $C_2D_4^{+\bullet}$ on Room-Temperature and Heated Carbon Surfaces

Juraj Jašík,[†,‡] Ján Žabka,[†] Linda Feketeová,[§,⊥] Imre Ipolyi,[†,‡] Tilmann D. Märk,[§] and Zdenek Herman*[,†,§]

V. Čermák Laboratory, J. Heyrovský Institute of Physical Chemistry, Academy of Sciences of the Czech Republic, Dolejškova 3, 182 23 Prague 8, Czech Republic, and Institut für Ionenphysik, Leopold-Franzens Universität, Techniker Strasse 25, A-6020 Innsbruck, Austria

Received: June 8, 2005; In Final Form: September 21, 2005

Interaction of $C_2H_n^+$ ($n = 2-5$) hydrocarbon ions and some of their isotopic variants with room-temperature and heated (600 °C) highly oriented pyrolytic graphite (HOPG) surfaces was investigated over the range of incident energies 11−46 eV and an incident angle of 60° with respect to the surface normal. The work is an extension of our earlier research on surface interactions of CH_n^+ ($n = 3-5$) ions. Mass spectra, translational energy distributions, and angular distributions of product ions were measured. Collisions with the HOPG surface heated to 600 °C showed only partial or substantial dissociation of the projectile ions; translational energy distributions of the product ions peaked at about 50% of the incident energy. Interactions with the HOPG surface at room temperature showed both surface-induced dissociation of the projectiles and, in the case of radical cation projectiles $C_2H_2^{+\bullet}$ and $C_2H_4^{+\bullet}$, chemical reactions with the hydrocarbons on the surface. These reactions were (i) H-atom transfer to the projectile, formation of protonated projectiles, and their subsequent fragmentation and (ii) formation of a carbon chain build-up product in reactions of the projectile ion with a terminal CH_3-group of the surface hydrocarbons and subsequent fragmentation of the product ion to $C_3H_3^+$. The product ions were formed in inelastic collisions in which the translational energy of the surface-excited projectile peaked at about 32% of the incident energy. Angular distributions of reaction products showed peaking at subspecular angles close to 68° (heated surfaces) and 72° (room-temperature surfaces). The absolute survival probability at the incident angle of 60° was about 0.1% for $C_2H_2^{+\bullet}$, close to 1% for $C_2H_4^{+\bullet}$ and $C_2H_5^+$, and about 3−6% for $C_2H_3^+$.

1. Introduction

Investigation of ion−surface collisions offers an opportunity to obtain information on a broad range of physical and chemical processes. Considerable attention has been devoted, especially in the past decade, to collisions of slow ions of energies of about 1−100 eV.[1−4] This energy regime is usually referred to as the hyperthermal energy range.[4] The collision energy in this range is comparable to or greater than typical bond energies, and the projectile ion incident energy is large enough to cause bond dissociation without obscuring the chemical nature of the interactions. Collisions of slow ions with surfaces find many applications in science and technology. They offer useful information on both projectiles (in particular polyatomic species) and surfaces, as well as on the characteristics of ion−surface interactions.

Ion−surface collisions can be a source of important data relevant to plasma-wall interactions in electrical discharges and fusion systems.[5] Hyperthermal plasma particles may collide with solid surfaces such as limiters and divertors in fusion devices, eroding the material by chemical and physical processes. Charged and neutral particles emitted from the surface may interact with the plasma and hit the surfaces again. In fusion devices, carbon is widely used as the material exposed to plasma and the outcome of collisions between ions and carbon surfaces is of considerable interest. Quite recently, the importance of interaction of molecular ionic species in the gaseous phase and in collisions with surfaces in fusion devices has been recognized, and demand for data on collisions of slow molecular ions, diatomic and simple polyatomic, has been repeatedly emphasized. The list of the molecular ion of importance in this respect contains, besides others, ions of C_1-C_3 group hydrocarbons, H_2O, CO, CO_2, BeH_n, and SiH_n.[6]

With our recent paper,[7] we started a systematic investigation of the interaction of small hydrocarbon ions (C_1-C_3) with carbon surfaces. We described the results of our scattering studies of small hydrocarbon ions (CD_5^+, $CD_4^{+\bullet}$, CD_3^+, and their H or ^{13}C isotopic variants) impinging on heated and nonheated highly oriented pyrolytic graphite (HOPG) surfaces. The experimental data consisted of results of measurements of mass spectra and angular and translational energy distributions of the ion products. Analysis of the data made it possible to estimate the ion survival probability and to describe the projectile fragmentation processes and chemical reactions with

* To whom correspondence should be addressed. E-mail: zdenek.herman@jh-inst.cas.cz.

[†] Academy of Sciences of the Czech Republic.

[‡] Pre-Doctoral Stipendist under the auspices of the EU Network MCI (Generation, Stability and Reaction Dynamics of Multiply charged Ions), 2002-2003. Home address: Department of Experimental Physics, Comenius University, Bratislava, Slovak Republic.

[§] Leopold-Franzens Universität.

[⊥] Visitor to the J. Heyrovský Institute under the cooperation programme Association EURATOM-IPP.CR and Association EURATOM-ÖAW.

10.1021/jp053064a CCC: $30.25
Published on Web 10/22/2005

the surface material. Collisions with room-temperature HOPG surfaces showed both surface-induced dissociation of the projectiles and chemical reactions with the surface material. The projectiles showed formation of $C_2X_3^+$ (X = H,D) in interaction of the projectiles with terminal CH_3 groups of surface-adsorbed hydrocarbons and formation of a small amount of C_3 product ions. Collisions of $CD_4^{+\bullet}$ led, in addition, to the formation of CD_4H^+ in a H-atom transfer reaction with hydrogen of surface hydrocarbons. The surface collisions were inelastic, with 41−55% of the incident energy in product ion translation. Heating of the surface to 600 °C practically removed the surface hydrocarbon layer as indicated by the absence of products of the efficient H-atom transfer reaction. Interactions of the projectiles with the heated surface showed only fragmentation of the projectile ions (no chemical reactions) in inelastic collisions with about 75% of the incident energy in product ion translation. The ion−surface scattering method used in these experiments was described earlier[8−12] in connection with estimation of energy partitioning in collisions of polyatomic ions with various surfaces, namely, surfaces covered by various self-assembled monolayers,[10] stainless steel covered by hydrocarbons,[8,9] and various carbon surfaces.[11]

Earlier work on ion−surface interaction of hydrocarbon ions includes studies of dissociation of small hydrocarbon, CH_n^+, and fluorocarbon, CF_n^+ (n = 1, 2, ...) ions on aluminum surfaces to gain insight into surface processes in plasma processing.[13] Significant charge neutralization (survival of about 0.3% for CH_n^+), dissociation of projectiles, and kinetic energies of fragments lower than 10 eV were observed for incident projectile energies up to 150 eV. In other studies, dissociative collisions of hydrogen ions (H_2^+, H_3^+, and their isotopic variants) on a hydrocarbon-covered stainless steel surface were investigated.[14] The effect of initial internal energy of hydrocarbon projectiles CH_n^+[15] and $C_2H_n^+$[16] on the extent of surface-induced fragmentation of the projectiles was studied, and it was found that the initial internal energy was fully available in the fragmentation process. Several papers were devoted to dissociative scattering of diatomic or small polyatomic (3−4 atoms) ions from single-crystal or liquid surfaces, including energy and angular analysis of the product ions. Negative ion formation in collisions of hyperthermal, state-selected NO^+ with O/Al(111)[17] and OCS^+ with Ag(111)[18] was investigated, and conclusions about the mechanism were made. Dissociative scattering of 50−250 eV fluorocarbon ions, CF_n^+ (n = 1−3), from surfaces covered by a perfluoropolyether liquid film[19−21] was interpreted on the basis of elastic scattering from the surface layer terminal group.

Changes in slow ion scattering and energy transfer for clean versus adsorbate-covered graphite surfaces were described for collisions of fullerene ions.[22] The extent of fragmentation, kinetic energy of the scattered ions, and chemical reactions (C_2 pick up on hydrocarbon-contaminated HOPG surface) changed dramatically after cleaning the surface by heating to 1000 °C. Examples of pick-up chemical reactions of incident ions with surface material have been described; the results have been summarized in reviews.[2,4] Significant changes in product ion kinetic energy distributions and the extent of incident-to-internal energy transfer were observed in scattering studies of $Si(CH_3)_3^+$ collisions with a clean Au(111) surface and a Au surface covered by a hydrocarbon C_6 self-assembled monolayer.[23]

In this paper, we extend our previous studies[7] of dissociative and reactive processes in hydrocarbon ion−carbon surface collisions to the investigation of $C_2H_n^+$ ions. Results of scattering experiments on collisions of $C_2H_2^{+\bullet}$ ($C_2D_2^{+\bullet}$), $C_2H_3^+$, $C_2H_4^{+\bullet}$ ($C_2D_4^{+\bullet}$), and $C_2H_5^+$ with room-temperature and heated (to 600 °C) surfaces of highly oriented pyrolytic graphite (HOPG) in the collision energy range 10−45 eV are reported. The ion survival probability for a series of projectile ions is determined, and surface-induced dissociation (SID) and chemical reactions with the surface material are identified from the measurements of mass spectra, translational energy, and angular distributions of the ion products.

2. Experimental Section

The experiments were carried out with the Prague beam scattering apparatus EVA II modified for ion−surface collision studies. The application of the apparatus to the described studies was described earlier.[7−12] In the present experiments, projectile ions were formed by bombardment by 120 eV electrons of acetylene, ethylene, or ethane (or their deuterated variants) at an ion source pressure of about 3×10^{-5} Torr. The ions were extracted, accelerated to about 150−200 eV, mass analyzed by a 90° permanent magnet, and decelerated to the required energy in a multielement deceleration lens. The resulting beam had an energy spread of 0.2 eV, full width at half-maximum (fwhm), angular spread of about 2°, fwhm, and geometrical dimensions of 0.4×1.0 mm^2. The beam was directed toward the carbon target surface under a preadjusted incident angle, Φ_N. Ions scattered from the surface passed through a detection slit (0.4×1 mm^2), located 25 mm away from the target, into a stopping potential energy analyzer. After energy analysis, the ions were focused and accelerated to 1000 eV into a detection mass spectrometer (a magnetic sector instrument), and detected with a Galileo channel multiplier. The primary beam exit slit, the target, and the detection slit were kept at the same potential during the experiments, and this equipotential region was carefully shielded by μ-metal sheets. The primary beam−target section could be rotated about the scattering center with respect to the detection slit to obtain angular distributions. The mass spectra of product ions were recorded with the stopping potential set at zero.

The energy of the projectile ions was measured by applying to the target a potential exceeding the nominal ion energy by about 10 eV. The target area then served as a crude ion deflector directing the projectile ions into the detection slit. Their energy could be determined with accuracy better than about 0.2 eV. The incident angle of the projectile ions was adjusted before an experimental series by a laser beam reflection with a precision better than 1°. Incident (Φ_N) and scattering (Θ'_N) angles were measured with respect to the surface normal.

The carbon surface target was a 5×5 mm^2 sample of highly oriented pyrolytic graphite (HOPG) from which the surface layer was peeled-off immediately before it was placed into vacuum. The sample was mounted into a stainless steel holder located 10 mm in front of the exit slit of the projectile ion deceleration system. The thickness of the sample holder made angular measurements at scattering angles smaller than about 3° of the surface parallel difficult (scattering angles 87°−90°). The carbon target surfaces in the experiments were kept either at room temperature or at an elevated temperature of about 600 °C. For this purpose, the carbon surface could be resistively heated to about 1000 K and its temperature measured by a thermocouple and by a pyrometer. Practical absence of chemical reactions with surface hydrocarbons indicated that heating the surface to 600 °C or higher decreased the concentration of hydrocarbons on the surface more than 100 times.[7] The temperature of 600 °C was thus regarded as sufficiently high to essentially remove the hydrocarbon layer that covered the HOPG surface at room temperature, and it was used in the present experiments (see

TABLE 1: Mass Spectra of Product Ions from Collisions of Projectile Ions with Carbon HOPG Surfaces Heated to 600 °C

energy		products [*m/z*]									
(eV)	projectile	13	15	18	25	26	27	28	29	30	32
11.3	$C_2H_2^+$					100					
31.3	$C_2D_2^+$							97.6	2.4		
	$C_2H_2^+$					100					
	$C_2H_3^+$					11.6	87.9	0.5			
	$C_2D_4^+$							22.3	0.9	66.8	10.0
	$C_2H_4^+$					18.0	49.0	32.0	1.0		
46.3	$C_2H_2^+$				7.3	90.7	2.0				
	$C_2H_3^+$					26.1	73.9				
	$C_2H_4^+$					22.7	75.2	2.1			

also sections 3.3 and 3.4). At higher temperatures, an increasing emission of K^+ ions from the sample was observed.

The scattering chamber of the apparatus was pumped by a 2000 L/s diffusion pump (Convalex polyphenyl ether pump fluid) and the detector by a 65 L/s turbomolecular pump; both pumps were backed by rotary vacuum pumps. The background pressure in the apparatus was about 5×10^{-7} Torr, during the experiments the pressure was about 5×10^{-6} Torr due to the leakage of the source gas into the scattering chamber.

3. Results and Discussion

3.1. Mass Spectra of Product Ions. Results of measurements of mass spectra of product ions from collisions of the projectile ions $C_2H_2^{+\bullet}$, $C_2D_2^{+\bullet}$, $C_2H_3^+$, $C_2H_4^{+\bullet}$, $C_2D_4^{+\bullet}$, and $C_2H_5^+$ with the HOPG surface heated to 600 °C are summarized in Table 1, those from collisions with the room-temperature (nonheated) HOPG surface are shown in Table 2. Ion intensities are presented as percent fractions of the total product ion intensity recorded at m/z 15−45, $I_{rel} = 100I_i/(\sum I_i)$. The spectra are shown at three incident energies, usually 16.3, 31.3, and 46.3 eV. The incident angle of the projectiles was $\Phi_N = 60°$ (i.e., 30° with respect to the surface). The spectra of product ions were measured at their angular maximum or close to it, for collision with the heated HOPG surface at 68° (22° with respect to the surface) and for collisions with the HOPG surface at room temperature at $\Theta'_N = 74°$ (i.e., 16° with respect to the surface). The relative ion intensities in Tables 1 and 2 are usually averages of a series of experimental runs.

The spectra from the carbon surface at room temperature (Table 2) show a considerable amount of product ions formed in chemical reactions with the surface material. The most prominent reaction is H-atom transfer with the projectile radical ions, $M^{+\bullet}$ ($C_2H_2^{+\bullet}$, $C_2D_2^{+\bullet}$, $C_2H_4^{+\bullet}$, $C_2D_4^{+\bullet}$), leading to the product ion MH^+. In addition, product ions $C_3X_n^+$ (X = H,D) can be observed in the spectra in lesser amounts. These ions either may result from sputtering of the surface material or may be formed in chemical reactions of the projectile with the surface material. Their origin and mechanism of their formation will be discussed in section 3.4. The mass spectra obtained in collisions of the projectile ions with the HOPG surface heated to 600 °C (Table 1) did not show products of the above-mentioned chemical reactions (protonated projectile formation or $C_3X_n^+$ formation) to any measurable extent. Therefore, we concluded, in agreement with our earlier findings,[7] that at room temperature the HOPG surface was covered by a layer of background hydrocarbons. When the surface was heated to 600 °C, this surface layer was effectively removed, and the collisions took place with a largely hydrocarbon-free graphite surface.

3.2. Ion Survival Probability. The ion survival probability, S_a, is the percentage of ions surviving the surface collision, and we define it as the sum of intensities of all ions scattered from the target, $\sum I_{PT}$, in relation to the intensity of the projectile reactant ions incident on the target, I_{RT}, $S_a = 100\sum I_{PT}/I_{RT}$. The quantities measured directly in the experiments are the current of the projectile ions incident on the surface, I_{RT}, and the ion currents of product ions reaching the detector, $\sum I_{PD}$. The equivalent current of all product ions scattered from the target surface, $\sum I_{PT}$, has to be estimated from $\sum I_{PD}$, the discrimination of the apparatus (D_A), and the angular discrimination of the scattering differential measurements ($D(\omega)$). The procedure used in the estimation of S_a was described in detail in our previous paper.[7] It leads to an expression for the absolute survival probability $S_a = 100FS_{eff}$, where the effective survival probability, $S_{eff} = \sum I_{PD}/I_{RT}$, contains the measurable quantities and the constant F summarizes all discrimination effects. From discrimination effects of the apparatus and from angular distributions of the projectile and product ions, we estimated for the present measurements $F = 0.29$ (including the multiplication factor of the multiplier), a value somewhat lower than that in our previous study of CH_n^+ ions (0.52).[7] Due to the approximations in estimating F, the values of S_a are presumably close to the upper limit of the ion survival probability. The values of S_a for collisions with both the room-temperature and heated surface, together with the relative error limits from

TABLE 2: Mass Spectra of Product Ions from Collisions of Projectile Ions with Carbon HOPG Surfaces at Room Temperature (Nonheated)

energy		products [*m/z*]																	
(eV)	projectile	15	18	26	27	28	29	30	31	32	33	37	38	39	40	41	42	43	45
11.3	$C_2H_2^+$			88.6	11.4														
	$C_2H_5^+$				33.7		66.3												
16.3	$C_2H_3^+$			4.6	94.0	1.2	0.1							0.1					
	$C_2H_4^+$	0.1		0.8	3.7	94.0	1.1	0.1						0.1		0.1			
	$C_2H_5^+$				63.5		36.5												
31.3	$C_2H_2^+$	1.3		35.4	48.5		2.4						2.4	8.0	0.5	1.5			
	$C_2H_3^+$			30.8	67.0									2.2					
	$C_2D_4^+$				1.5	15.5	16.7	42.5	0.8	1.2	17.8			0.6	0.8	1.8	0.8		
	$C_2H_4^+$	0.3		14.6	63.5	2.6	14.7							3.1		1.2			
	$C_2H_5^+$	1.1		3.0	88.1	1.8	4.4							1.1		0.5			
46.3	$C_2D_2^+$			4.8	32.0	20.0	26.5	2.2					1.6	5.6	3.6	3.2	0.5		
	$C_2H_2^+$	1.6		39.2	41.0		1.9						3.9	11.5		0.9			
	$C_2H_3^+$			49.5	47.4									1.8		1.3			
	$C_2D_4^+$		0.5	0.8	7.0	26.8	15.3	38.9	0.5	0.7	0.5		0.7	2.1	2.2	3.4	0.6		
	$C_2H_4^+$	0.7		25.1	57.7	2.5	4.5							6.5		3.0			
	$C_2H_5^+$	1.8		12.0	79.0	3.9								2.3		1.0			

TABLE 3: Percentage of Surviving Ions, S_a (%), in Collisions of CH_n^+ and $C_2H_n^+$ Ions with Room-Temperature (Nonheated) and Heated HOPG Surfaces

	E_{inc} (eV)			
projectile	11.7	16.3	31.3	46.3
		Nonheated		
CD_3^+ [a]		*0.12 ± 0.03*	*0.22 ± 0.04*	*0.26 ± 0.16*
$CD_4^{+\bullet}$ [a]		*0.37 ± 0.06*	*0.34 ± 0.2*	*0.27 ± 0.26*
CD_5^+ [a]		*12.5 ± 5*	*12.0 ± 5*	*18 ± 7*
$C_2H_2^{+\bullet}$	0.1 ± 0.03		0.1 ± 0.03	0.06 ± 0.01
$C_2D_2^{+\bullet}$				0.08 ± 0.02
$C_2H_3^+$		6.4 ± 0.4	4.1 ± 0.7	2.4
$C_2H_4^{+\bullet}$		2.3 ± 0.6	1.2	0.7 ± 0.1
$C_2D_4^{+\bullet}$			1.0 ± 0.4	0.9 ± 0.2
$C_2H_5^+$	0.3 ± 0.03	1.1 ± 0.03	1.0 ± 0.1	0.3 ± 0.03
		Heated		
CD_3^+ [a]		*0.09*		*0.1*
$CD_4^{+\bullet}$ [a]		*(5)*	*2.3*	
CD_5^+ [a]				*23*
$C_2H_2^{+\bullet}$	0.1 ± 0.04		0.1 ± 0.04	0.36
$C_2D_2^{+\bullet}$			0.07 ± 0.2	
$C_2H_3^+$			3.6 ± 0.2	5
$C_2H_4^{+\bullet}$			0.2 ± 0.05	0.8 ± 0.2
$C_2D_4^{+\bullet}$			0.4 ± 0.05	

[a] Data from ref 7.

repeated determinations, are summarized in Table 3. For comparison, we include in this table our data for S_a of CH_n^+ ($n = 3-5$) ions (in italics), published earlier.[7]

The values of the survival probability are in general agreement with our earlier findings[7,8] showing considerable differences for S_a values of different ions. The survival probability of $C_2H_2^{+\bullet}$ ($C_2D_2^{+\bullet}$) ions was found to be about 0.1%, for $C_2H_4^{+\bullet}$ and $C_2H_5^+$ it was close to 1%, and for $C_2H_3^+$ it was 3−6%. The values of the survival probability did not exhibit a clear dependence on the incident energy, and they were similar on heated ("clean") and room-temperature (hydrocarbon-covered) carbon surfaces.

3.3. Product Ions from Collisions with the Heated HOPG Surface. Results on collisions of the projectile ions with the HOPG surface heated to 600 °C represent a simpler case than those for the room-temperature surface. The mass spectra of product ions are summarized in Table 1. Only a limited number of mass spectra were measured at collision energies of 11.3, 31.3, and 46.3 eV. The mass spectra are rather simple, showing only surface-induced dissociation of the product ions at higher collision energies. No products of chemical reactions with the surface material could be detected.

The projectile ion $C_2H_2^{+\bullet}$ ($C_2D_2^{+\bullet}$) remains undissociated at lower collision energies, and only at the highest collision energy of 46.3 eV, it shows partial fragmentation (of about 8%) to C_2H^+ (C_2D^+) by a loss of H(D). The projectile ion $C_2H_3^+$ dissociates partly by a loss of a H-atom to $C_2H_2^{+\bullet}$ (11% and 26% at 31.3 and 46.3 eV, respectively). The main dissociation processes of the cation $C_2H_4^{+\bullet}$ upon surface collision excitation are a loss of H and a loss of H_2 to form $C_2H_3^+$ and $C_2H_2^{+\bullet}$ products, respectively, at increasing amounts with increasing incident energy. At 46.3 eV, only about 2% of the projectile ions remain undissociated. No measurable amounts of fragmentation to CH_n^+ (CH_3^+, CH_2^+) could be detected. The data are in over-all agreement with the break-down patterns of the molecular ions $C_2H_2^{+\bullet}$ and $C_2H_4^{+\bullet}$.

Unfortunately, estimation of translational-to-internal energy transfer and determination of $P(E'_{int})$, as carried out for collisions of other projectiles in our previous papers,[7,8,10,12] could not be done for the projectiles studied in this paper. The break-down patterns or other relevant data necessary for it are not available for $C_2H_3^+$ and $C_2H_5^+$; in case of $C_2H_2^{+\bullet}$, the stability of the molecular ion over more than 4 eV above the internal energy (IE) does not provide enough variation to calculate reliable $P(E'_{int})$. In the case of $C_2H_4^{+\bullet}$ formed by electron ionization of ethylene, the molecular ion has a complicated initial internal energy content (two regions of internal energy, between 0 and 0.5 eV and between 2 and 2.7 eV, see Figure 7 in ref 16), and this made an estimation of $P(E'_{int})$ ambiguous.

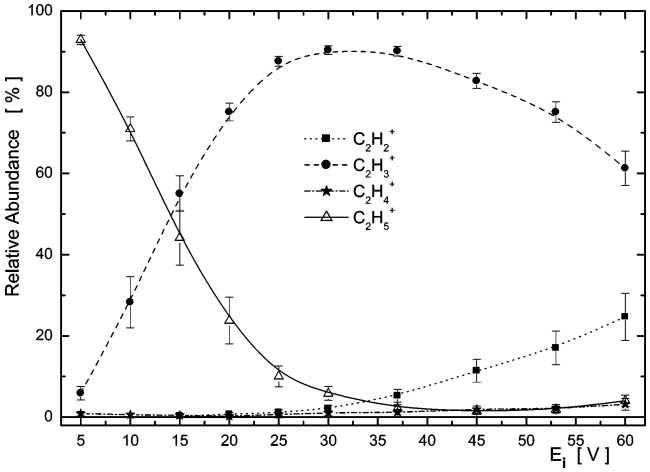

Figure 1. Dependencies of the relative abundance of product ions on the incident energy for the projectile ion $C_2H_5^+$: CERMS (collision-energy resolved mass spectra) curves for projectile and fragment ions scattered from the room-temperature HOPG surface.

3.4. Product Ions from Collisions with the HOPG Surface at Room Temperature (Nonheated)−Chemical Reactions with the Surface Material. Mass spectra of product ions from collisions of the projectile ions $C_2H_2^{+\bullet}$, $C_2D_2^{+\bullet}$, $C_2H_3^+$, $C_2H_4^{+\bullet}$, $C_2D_4^{+\bullet}$, and $C_2H_5^+$ with the HOPG surface at room temperature are shown in Table 2 for several collision energies between 11.3 and 46.3 eV. The spectra differ from those obtained with the heated surface in that they show also contributions of ions at masses higher than the mass of the projectile ion. In the spectra of product ions from collisions of closed-shell ions $C_2H_3^+$and $C_2H_5^+$, the simple dissociation of the surface-excited projectile ions prevails. For these projectiles, very small amounts of ions of *m*/*z* 39 ($C_3H_3^+$) and 41 ($C_3H_5^+$) were formed in a ratio of about [39]/[41] ≈ 2−3 at incident energies of 31.3 and 46.3 eV. Use of deuterated projectiles indicated that these ions resulted from sputtering of the surface material induced by those closed-shell ion projectiles.

For the projectile ion $C_2H_5^+$, the dependence of the relative abundance of product ions on the incident energy of the projectile was measured in more detail, and the collision energy resolved mass spectra (CERMS curves) were obtained. The data are shown in Figure 1. The CERMS curves are in very good agreement with the CERMS curves obtained earlier in Innsbruck with a different apparatus for collisions of the $C_2H_5^+$ projectile with a stainless steel surface covered at room temperature with hydrocarbons.[16] This agreement indicates that the surface hydrocarbon layer determines prevailingly the behavior of the surface in surface-induced dissociation.

In collisions of the radical cations $C_2H_2^{+\bullet}$ and $C_2H_4^{+\bullet}$ (and their isotopic variants) with the HOPG at room temperature, the product ions evidently result both from simple dissociation of the projectile and from chemical reactions with hydrocarbons on the surface. The most prominent chemical reaction is H-atom transfer from the surface hydrocarbons to the radical cations, leading to the formation of the protonated projectile $C_2H_3^+$

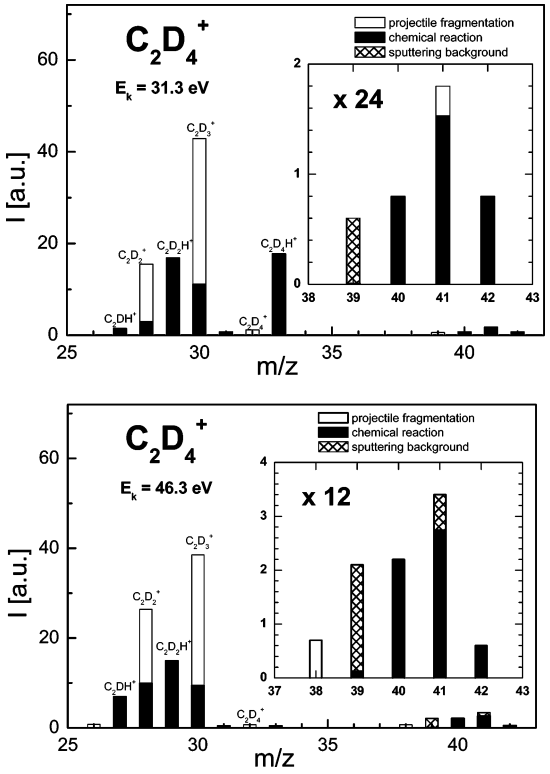

Figure 2. Analysis of the contributions to the mass spectrum of product ions from collisions of $C_2D_4^{+\bullet}$ projectiles with the HOPG surface at room temperature: (a) $E_i = 31.3$ eV; (b) $E_i = 46.3$ eV. See also the mass spectra in Table 2. Columns represent measured ion intensities; open sections represent fragmentation of the projectile ion; black represents contributions from chemical reactions; crosshatching represents sputtering background. For details, see text.

($C_2D_2H^+$) in reactions with $C_2H_2^{+\bullet}$ ($C_2D_2^{+\bullet}$) and $C_2H_5^+$ ($C_2D_4H^+$) in reactions of $C_2H_4^{+\bullet}$ ($C_2D_4^{+\bullet}$) and further decomposition of these products. Formation of ions of the C_3 group is less probable than protonation, but the abundance of ions of *m*/*z* 38−45 is visibly larger than in case of impact of the closed-shell cations $C_2H_3^+$ and $C_2H_5^+$, and intensities at particular masses differ considerably for collisions of hydrogenated and deuterated projectiles. This suggests that the C_3 product ions can originate both from sputtering of the surface constituents and from chemical reactions of carbon chain build-up with the surface material, the differences for impact of hydrogenated and deuterated projectiles being due to formation of partially deuterated ions of the group $C_3X_n^+$ (X = H,D).

Analysis of the $C_2X_n^+$ and $C_3X_n^+$ (X = H,D) group in the spectra of $C_2D_4^{+\bullet}$ at incident energies 46.3 and 31.3 eV is shown in Figure 2a,b. There were no detectable amounts of ions at masses above *m*/*z* 43. The sputtered ion background was obtained by detailed analysis of many spectra of different ions, and it was found to involve mostly contributions at *m*/*z* 39 ($C_3H_3^+$) and 41 ($C_3H_5^+$). At the above-mentioned incident energies, the ratio of sputtered ion intensities [*I*(39)]/[*I*(41)] was estimated at close to 3. By subtraction of the sputtered contributions, the ratio of $C_3X_n^+$ ions at *m*/*z* 39/40/41/42 was found to be 0.05:0.25:0.49:0.25 at the incident energy of 31.3 eV (Figure 2a) and 0.03:0.39:0.51:0.10 at the incident energy of 46.3 eV (Figure 2b). These ratios are consistent, within the experimental error, with statistical distribution of ions $C_3X_3^+$ (X = H,D) formed from an intermediate $C_3D_4H_3^+$ by subsequent emission of two X_2 molecules (the statistical ratio being 39/40/41/42 = 0.03:0.35:0.51:0.11).

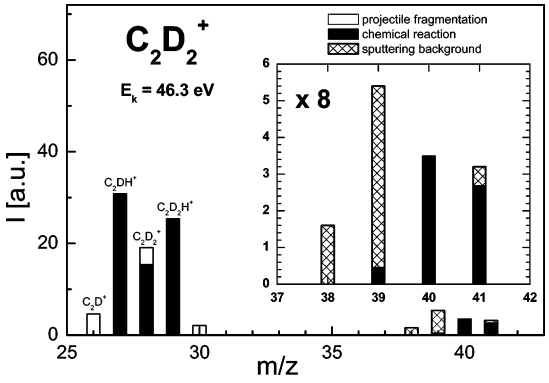

Figure 3. Analysis of the contributions to the mass spectrum of product ions from collisions of $C_2D_2^{+\bullet}$ projectiles with the HOPG surface at room temperature at $E_i = 46.3$ eV (see also mass spectrum in Table 2). Columns indicate measured ion intensities; open sections represent fragmentation of the projectile ion; black represents contributions from chemical reactions; crosshatching represents sputtering background. For details, see text.

The data suggest that the chemical reaction leading to $C_3X_n^+$ ions concerns interaction of the ethylene projectile with the terminal CH_3 group of the surface hydrocarbons, formation of a $C_3D_4H_3^+$ primary product ion, and its fragmentation by subsequent dissociation of two X_2 units to the most stable final product ion $C_3X_3^+$ (X = H,D), namely,

$$C_2D_4^{+\bullet} + CH_3\text{-}CH_2\text{-}S \rightarrow [C_3D_4H_3^+] + (CH_2^{\bullet}\text{-}S) \rightarrow C_3X_5^+ + X_2 \rightarrow C_3X_3^+ + X_2 \qquad (X = H,D) \quad (1)$$

This hypothesis was confirmed by analysis of the $C_3X_n^+$ group of product ions from collisions of $C_2D_2^{+\bullet}$ with the room-temperature carbon surface at the incident energy of 46.3 eV. The data and analysis are given in Figure 3. The final ratio of ion abundance at masses 39/40/41 was found to be 0.07:0.53:0.4, which is close to the statistical ratio 0.1:0.6:0.3 expected for an interaction of the incident ion $C_2D_2^{+\bullet}$ with the surface hydrocarbon terminal CH_3 group, formation of a primary product ion $C_3D_2H_3^+$, and its dissociation to $C_3X_3^+$ by release of X_2 (X = H,D).

The ratio of probabilities for different processes, namely, direct dissociation (DD) vs H-atom transfer (HT) vs C_3 reaction (CR), was DD/HT/CR = 1:1:0.1 for $C_2D_4^{+\bullet}$ collisions at 46.3 and 31.3 eV and DD/HT/CR = 0.1:1:0.1 for $C_2D_2^{+\bullet}$ at 46.3 eV.

It may be expected that formation of radical sites on the hydrocarbon surface after the H-atom transfer, eq 1, will eventually lead to formation of multiple bonds in the surface hydrocarbons. However, the described experiments provide no direct information on surface changes upon impact of the projectiles. This question was addressed earlier in valuable studies of growth and erosion of hydrocarbon films on surfaces upon interaction with hydrocarbon radicals or with hydrocarbon plasma.[24−27] Indeed, formation of multiple bonds on surfaces was observed in these investigations.

3.5. Translational Energy Distributions of Product Ions. Translational energy distributions of product ions were measured both for heated and for room-temperature surfaces. Within the experimental error, the velocity distributions of scattered undissociated projectile ions and of the major fragment ions peaked at the same velocity, and they were very similar. This indicates, in agreement with our earlier findings,[7−12] that the surface-induced fragmentation of the projectile ions takes place prevailingly after the interaction with the surface in an unimolecular way.

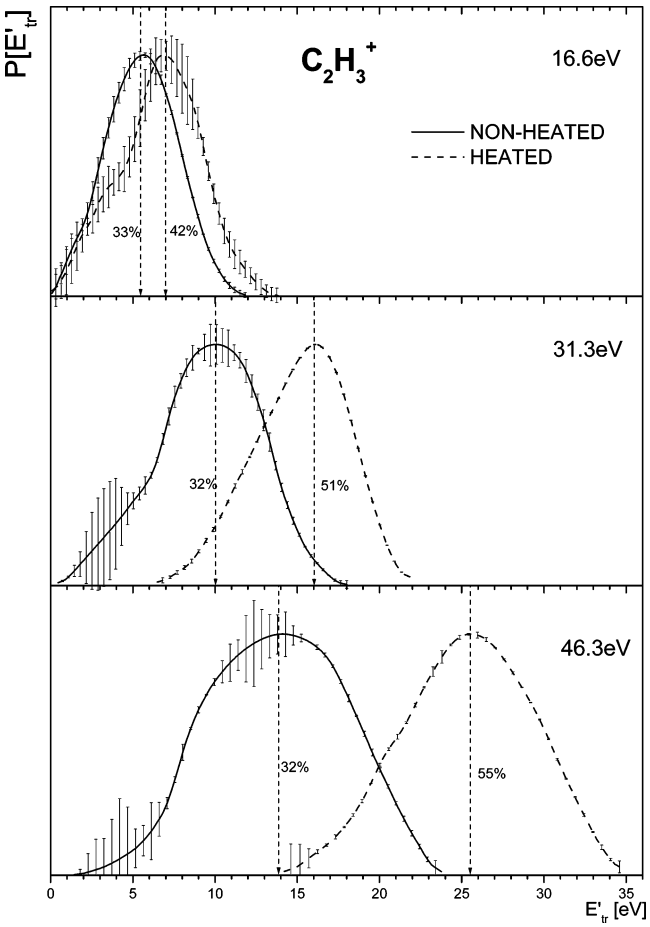

Figure 4. Translational energy distributions of the product ions $C_2H_3^+$ from collisions of $C_2H_3^+$ with (a) nonheated (room-temperature) HOPG surface (solid lines) and (b) HOPG surface heated to 600 °C (dashed lines) at incident energies of 16.6, 31.3, and 46.3 eV. Incident angle $\Phi_N = 60°$; numbers indicate peak energy of the distributions in % of the incident energy.

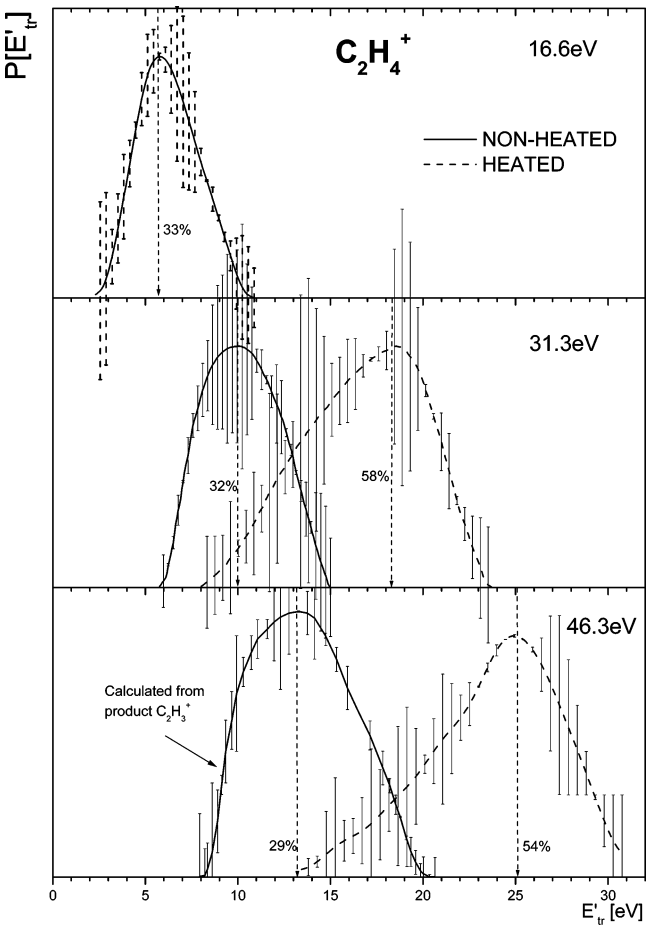

Figure 5. Translational energy distributions of the product ions $C_2H_4^+$ from collisions of $C_2H_4^+$ with (a) nonheated (room-temperature) HOPG surface (solid lines) and (b) HOPG surface heated to 600 °C (dashed lines) at incident energies of 16.6, 31.3, and 46.3 eV. Incident angle $\Phi_N = 60°$; numbers indicate peak energy of the distributions in % of the incident energy.

Translational energy distributions of typical scattered nondissociated projectile ions are shown in Figures 4−6 for ions scattered from heated (dashed lines) and room-temperature (solid lines) HOPG surfaces. The data are shown for three different incident energies between 11.3 and 46.3 eV. Figure 4 shows results for $C_2H_3^+$, Figure 5 for $C_2H_4^{+\bullet}$, and Figure 6 for $C_2H_5^+$. At the incident energy of 46.3 eV, where the abundance of the projectile ions among the products was negligible, translational energy distribution of the scattered projectile was recalculated from the translational energy distribution of a fragment ion assuming the same velocity distribution, that is, the postcollision unimolecular dissociation (namely, $C_2H_4^{+\bullet}$or $C_2H_5^+$ at 46.3 eV from $C_2H_3^+$, see Figures 5 and 6).

The data in Figures 4−6 clearly show that the product ions are formed in inelastic collisions with the surface. However, there is a substantial difference in the inelasticity of scattering from heated and room-temperature HOPG surfaces. For heated (i.e., hydrocarbon-free) HOPG surfaces, the inelastically scattered undissociated projectiles exhibit distributions peaking at translational energies of 50% ± 8% of the incident energy. On room-temperature surfaces (HOPG covered with hydrocarbons), the peak of the translational energy distributions lies at 31% ± 4% of the incident energy (the only exception is $C_2H_5^+$ at 46.3 eV, calculated from $C_2H_3^+$ translational energy distribution, where the rather broad distribution peaks at 41% of the incident energy). The room-temperature, hydrocarbon-covered HOPG surface behaves therefore as a somewhat "softer" surface than the heated HOPG surface. This behavior is analogous to our findings for collisions of hydrocarbon ions CH_n^+ ($n = 3-5$).[7] However, surface collisions of these smaller projectiles were less inelastic: with the heated HOPG, the translational energy of products was about 75% of the incident energy, and with the room-temperature surface, it was about 41−55%, at the same incident angle.[7]

3.6. Angular Distributions of Product Ions. A summary of angular distribution data for different projectile ions scattered from heated and nonheated HOPG surfaces at different incident energies is shown in Figure 7. In all cases, the incident angle was $\Phi_N = 60°$ (30° with respect to the surface, see Figure 7). The data are given as polar plots separately for heated and nonheated surfaces for three incident energies of 21.3, 31.3, and 46.3 eV. Because angular distributions of different product ions on the same surface and at the same incident energy were very similar, data for different ions are given in one picture (Figure 7). However, there is some difference in peaking of the angular distributions of product ions scattered from the heated ($\Theta'_N \approx 67°-68°$, i.e., 22°−23° with respect to the surface) and room-temperature surface ($\Theta'_N \approx 72°-75°$, i.e., 15°−18° with respect to the surface). The widths of the angular distributions are about the same for both heated and room-temperature surfaces (about 17°−20°, full width at half-maximum).

In our previous papers[8,10] we analyzed the projectile and product velocity−angle relations (peak values) for different incident angles in terms of projectile and product ion velocity

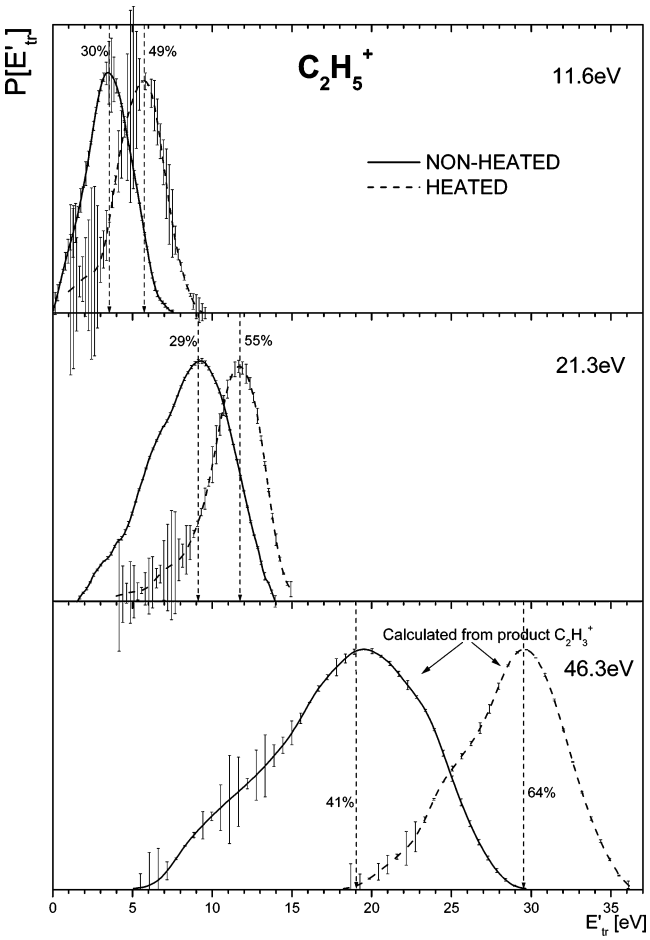

Figure 6. Translational energy distributions of the product ions $C_2H_5^+$ from collisions of $C_2H_5^+$ with (a) nonheated (room-temperature) HOPG surface (solid lines) and (b) HOPG surface heated to 600 °C (dashed lines) at incident energies of 11.6, 21.3, and 46.3 eV. Incident angle $\Phi_N = 60°$; numbers indicate peak energy of the distributions in % of the incident energy.

components parallel and perpendicular to the surface. It turned out that the ratio of parallel velocities of product (v_1') and projectile (v_1) ion, (v_1'/v_1), was the same for a variety of surfaces for different incident angles and different incident energy and equal to 0.7 ± 0.1. The perpendicular velocity component of the product ions, v_2', was independent of the incident angle and increased linearly with incident energy. For room-temperature, hydrocarbon-covered surfaces and projectile (ethanol cation) energy of 22.3 eV, it was 2.6 ± 0.2 km/s;[8] for a surface covered by a hydrocarbon C_{12} SAM (self-assembled monolayer) and the same incident energy, it was 1.5−2 km/s.

The present experiments provide data for three incident energies but only for one incident angle, 60°. The available data for $C_2H_5^+$ and $C_2H_3^+$ (Figures 4, 6, and 7) give for the room-temperature HOPG surface $v_1'/v_1 = 0.66$ and for the heated surface $v_1'/v_1 = 0.78$, in reasonably good agreement with the above-mentioned value for all systems studied so far. The value of v_2' for the room-temperature HOPG surface increased between incident energies 21 and 46 eV from 2.1 to 3.1 km/s, the former value being in good agreement with the above-mentioned value of v_2' for hydrocarbon-covered surfaces. However, for the heated, hydrocarbon-free HOPG surface, the respective value of v_2' was by a factor of 1.7 larger than that for room-temperature surface, increasing from 3.3 to 5.3 km/s for incident energies from 21 to 46 eV. This suggests a "mattress" effect in the perpendicular velocity component of the product ions depending on the quality of the surface. The question will

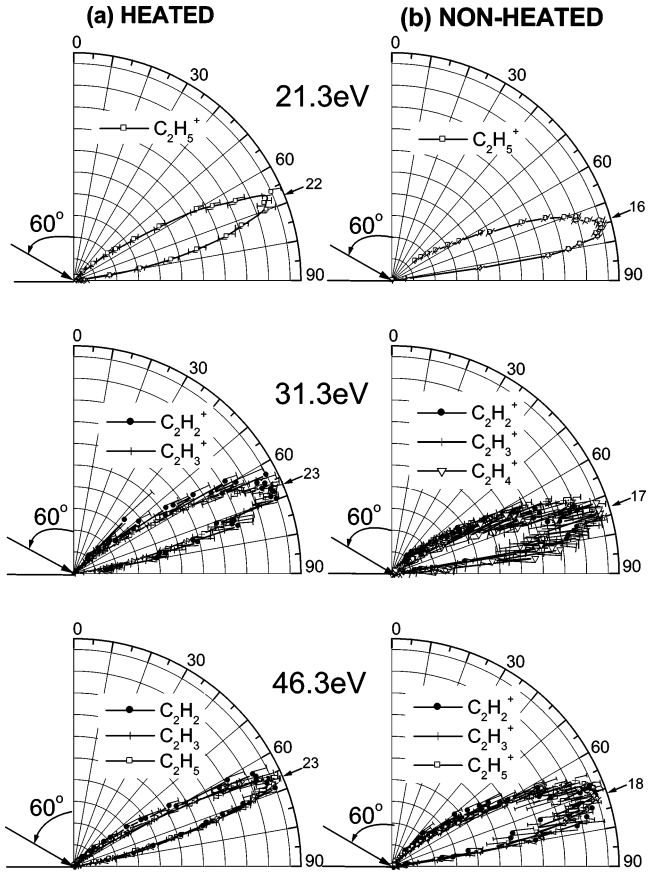

Figure 7. Polar plots of angular distributions of product ions (inelastically scattered undissociated projectile ions as indicated in the figure) from collision with heated (left) and nonheated (right) HOPG surfaces at incident energies of the projectiles of 21.3, 31.3, and 46.5 eV. Incident angle $\Phi_N = 60°$; arrows indicate peaks of angular distributions.

be discussed more in detail in connection with our forthcoming data for C_3 hydrocarbons.

4. Conclusions

(1) Interaction of $C_2H_n^+$ ($n = 2-5$) hydrocarbon ions and some of their isotopic variants with room-temperature and heated (to 600 °C) HOPG surfaces was investigated over the range of incident energies, 11−46 eV, and at an incident angle of 60° (with respect to the surface normal). Mass spectra, translational energy distributions, and angular distributions of product ions were measured. This work is an extension of our earlier work on surface interactions of CH_n^+ ($n = 3-5$) projectile ions.[7]

(2) Collision with the heated HOPG surface led only to surface-induced dissociation processes of the projectile ions; product ions were formed in inelastic collision with the peak of the translational energy distribution at about 50% of the incident energy. In comparison with surface interactions of CH_n^+ ions (peak of E_{tr}' at about 75% of the incident energy), the collisions of $C_2H_n^+$ projectiles were thus more inelastic. Both nondissociated scattered projectiles and fragment product ions had very similar velocity distribution indicating that the fragmentation of the surface-excited projectiles took place prevailingly after the interaction with the surface in a unimolecular way.

(3) Collisions of the projectile ions with the HOPG surface at room temperature showed both dissociation of the projectile ion and, in case of radical cations, chemical reactions with the surface material. Translational energy distributions of the

inelastically scattered projectiles peaked at about 31% of the incident energy. Thus the collisions with the HOPG surface at room temperature were considerably more inelastic than those with the heated HOPG surface. This is analogous to our previous data on CH_n^+ projectiles, where, however, the translational energy of product ions peaked at 45−55% of the incident energy.

(4) Chemical reactions of the radical cation projectiles with the HOPG surface at room temperature showed processes of H-atom transfer from the surface material and formation of protonated projectiles and, to a lesser extent, reactions of carbon chain build-up, namely, formation of $C_3X_n^+$ ions. Isotopic analysis of $C_3X_n^+$ (X = H,D) products from collisions of $C_2D_4^{+\bullet}$ and $C_2D_2^{+\bullet}$ showed that the main product ion was $C_3X_3^+$ formed in interactions of the projectile with terminal CH_3 groups of the surface material and subsequent fragmentation of the primary product by X_2 dissociation. No reaction products $C_4H_n^+$ could be detected. Analogous reactions were observed in surface interactions of the CH_n^+ projectiles (H-atom transfer, formation of $C_2H_n^+$ product ions in interaction with the terminal CH_3 group of surface hydrocarbons).

(5) Chemical reactions in collisions with the room temperature HOPG surface showed, in agreement with our earlier findings, that the surface was covered with hydrocarbons. This surface layer could be effectively removed by heating the surface to about 600 °C or higher, as indicated by the lack of occurrence of the H-atom transfer reaction with radical cations in the case of heated surfaces.

(6) Angular distributions of the product ions were very similar for all measured projectiles over the investigated incident energy range. The angular distribution in collisions with the heated surface peaked at about 78° and for the surface at room-temperature somewhat closer to the surface, close to 72°−74°. The average angular width of these distributions was very similar, about 17°−20° (full width at half-maximum).

(7) The data made it possible to estimate the survival probability of the projectile ions. At the incident angle $\Phi_N = 60°$, the absolute survival probability, S_a, was estimated as about 0.1% for projectiles $C_2H_2^{+\bullet}$ and $C_2D_2^{+\bullet}$, close to 1% for $C_2H_4^{+\bullet}$, $C_2D_4^{+\bullet}$, and $C_2H_5^+$, and 3−6% for $C_2H_3^+$.

Acknowledgment. Partial support of this research by a grant of the Grant Agency of the Academy of Sciences of the Czech Republic (No. 4040405), by the Program of the Academy of Sciences (No. K4040110), by the Research Center (No. LC-510), by the Association EURATOM-IPC.CR in cooperation with Association EURATOM-ÖAW, and by the EU Network MCI (Generation, Stability and Reaction Dynamics of Multiply-Charged Ions) is gratefully acknowledged. The content of the publication is the sole responsibility of its authors, and it does not necessarily represent the views of the EU Commission or its services. One of the authors (Z.H.) wishes to express his gratitude to the Leopold-Franzens Universität in Innsbruck for a Visiting Professorship (2005) during which part of this manuscript was prepared.

References and Notes

(1) Rabalais, J. W., Ed. *Low Energy Ion-Surface Interactions*; J. Wiley: New York, 1994.
(2) Cooks, R. G.; Ast, T.; Mabud, M. D. *Int. J. Mass Spectrom*. **1990**, *100*, 209.
(3) Hanley, L., Ed. Polyatomic Ion-Surface Interactions. *Int. J. Mass Spectrom*. **1998**, *174*.
(4) Grill, V., Shen, J.; Evans, C.; Cooks, R. G. *Rev. Sci. Instrum*. **2001**, *72*, 3149.
(5) Hofer, W. O., Roth, J., Eds. *Physical Processes of the Interaction of Fusion Plasmas with Solids*; Academic Press: San Diego, CA, 1996.
(6) Unpublished data from IAEA Research Coordination Group "Data for molecular processes in edge plasmas", IAEA, Vienna, 2003.
(7) Roithová, J.; Žabka, J.; Dolejšek, Z.; Herman, Z. *J. Phys. Chem. B* **2002**, *106*, 8293.
(8) Kubišta, J.; Dolejšek, Z., Herman, Z. *Eur. Mass Spectrom*. **1998**, *4*, 311.
(9) Wörgötter, R.; Kubišta, J.; Žabka, J.; Märk, T. D.; Herman, Z. *Int. J. Mass Spectrom. Ion Processes* **1998**, *174*, 53.
(10) Žabka, J.; Dolejšek, Z.; Herman, Z. *J. Phys. Chem. A* **2002**, *106*, 10861.
(11) Žabka, J.; Dolejšek, Z.; Roithová, J.; Grill, V.; Märk, T. D.; Herman, Z. *Int. J. Mass Spectrom.* **2002**, *213*, 145.
(12) Herman, Z. *J. Am. Soc. Mass Spectrom.* **2003**, *14*, 1360.
(13) Sugai, H.; Mitsuoka, Y.; Toyoda, H. *J. Vac. Sci. Technol., A* **1998**, *16*, 290.
(14) Quayyum, A.; Mair, C.; Schustereder, W.; Scheier, P.; Hess, W.; Märk, T. D. *Chem. Phys. Lett.* **2003**, *372*, 166
(15) Qayyum, A.; Tepnual, T.; Mair, C.; Matt-Leubner, S.; Scheier, P.; Herman, Z.; Märk, T. D. *Chem. Phys. Lett*. **2003**, *376*, 539.
(16) Qayyum, A.; Herman, Z.; Tepnual, T.; Mair, C.; Matt-Leubner, S.; Scheier, P.; Märk, T. D. *J. Phys. Chem. A* **2004**, *108*, 1.
(17) Morris, J. R.; Kim, G.; Barstis, T. L. O.; Mitra, R.; Jacobs, D. C. *J. Chem. Phys.* **1997**, *107*, 6448.
(18) Maazous, M.; Barstis, T. L. O.; Maazous, P. L.; Jacobs, D. C. *Phys. Rev. Lett.* **2000**, *84*, 1331.
(19) Koppers, W. R.; Beijersbergen, J. H. M.; Weeding, T. L.; Kistemaker, P. G.; Kleyn, A. W. *J. Chem. Phys*. **1997**, *107*, 10736.
(20) Koppers, W. R.; Gleeson, M. A.; Lourenco, J.; Weeding, T. L.; Los, J.; Kleyn, A. W. *J. Chem. Phys.* **1999**, *110*, 2588.
(21) Los, J.; Gleeson, M. A.; Koppers, W. R.; Weeding, T. L.; Kleyn, A. W. *J. Chem. Phys.* **1999**, *111*, 11080.
(22) Beck, R. D.; Rockenberger, J.; Weiss, P.; Kappes, M. M. *J. Chem. Phys.* **1996**, *104*, 3638.
(23) Wainhaus, S. B.; Lim, H.; Schultz, D. G.; Hanley, L. *J. Chem. Phys.* **1997**, *106*, 10329.
(24) Hopf. C.; Letourner, K.; Jacob, W.; Schwarz-Selinger, T.; von Keudell, A. *Appl. Phys. Lett.* **1999**, *74*, 3800.
(25) Schwarz-Selinger, T.; von Keudell, A.; Jacob, W. *J. Appl. Phys.* **1999**, *86*, 3988.
(26) Hopf, C.; von Keudell, A.; Jacob, W. *Nucl. Fusion* **2002**, *42*, L27.
(27) Hopf, C.; von Keudell, A.; Jacob, W. *J. Appl. Phys.* **2003**, *93*, 3352.